



Article

Voltammetric Detection of Irbesartan by Molecularly Imprinted Polymer (MIP)-Modified Screen-Printed Electrodes

Camilla Zanoni ¹, Riccardo Rovida ¹ , Lisa Rita Magnaghi ^{1,2} , Raffaella Biesuz ^{1,2} and Giancarla Alberti ^{1,*} 

¹ Department of Chemistry, University of Pavia, Via Taramelli 12, 27100 Pavia, Italy

² Consorzio Interuniversitario Nazionale per la Scienza e Tecnologia dei Materiali (INSTM)-Unità di Ricerca di Pavia, Via G. Giusti 9, 50121 Firenze, Italy

* Correspondence: galberti@unipv.it

Abstract: Irbesartan is a drug used to treat hypertension and high blood pressure. Recent studies associated sartans with several forms of cancer, making removing this class of substances from the environment a high priority. The EU has categorized drugs as emerging pollutants, and they can be more potent than other substances because they were designed to operate at low concentrations. Thus, effective and sensitive methods of determining Irbesartan selectively and accurately in environmental samples are necessary. MIPs have already been used to remove pollutants from complex matrixes, so they were also chosen for this work. In particular, a polyacrylate-based MIP was used to functionalize the graphite working electrode of screen-printed cells (SPCs), aiming to develop a voltammetric method for Irbesartan sensing. The MIP composition and the experimental conditions for the electrochemical determination were optimized through a Design of Experiments (DoE) approach. The whole analysis was replicated with different SPCs obtaining similar results, which highlight the good reproducibility potential. MIP-based electrodes were also applied to determine Irbesartan in fortified tap water samples, obtaining high recovery percentages. Given the good results, the electrochemical method based on MIP-modified screen-printed electrodes is promising for quantifying Irbesartan at a trace level.

Keywords: Irbesartan; sartans drugs; emerging pollutants detection; molecularly imprinted polymers (MIPs); MIP-modified electrodes; screen-printed electrodes; electroanalysis; analytical chemistry; Design of Experiments; Square-Wave Voltammetry



Citation: Zanoni, C.; Rovida, R.; Magnaghi, L.R.; Biesuz, R.; Alberti, G. Voltammetric Detection of Irbesartan by Molecularly Imprinted Polymer (MIP)-Modified Screen-Printed Electrodes. *Chemosensors* **2022**, *10*, 517. <https://doi.org/10.3390/chemosensors10120517>

Academic Editors: Yi Wang and Xingchu Gong

Received: 12 November 2022

Accepted: 5 December 2022

Published: 6 December 2022

Publisher's Note: MDPI stays neutral with regard to jurisdictional claims in published maps and institutional affiliations.



Copyright: © 2022 by the authors. Licensee MDPI, Basel, Switzerland. This article is an open access article distributed under the terms and conditions of the Creative Commons Attribution (CC BY) license (<https://creativecommons.org/licenses/by/4.0/>).

1. Introduction

Irbesartan, (IUPAC name: 2-butyl-3-((4-[2-(2H-1,2,3,4-tetrazol-5-yl)phenyl]phenyl)methyl)-1,3-diazaspiro [4.4]non-1-en-4-one, see Figure 1), is a potent and selective angiotensin II receptor antagonist recommended for use in patients with hypertension and those with type 2 diabetes mellitus and nephropathy [1,2].

The EU has classified many drugs, including sartans, as “emerging pollutants,” substances whose effects on the environment and the human population in the short and the long term have not been thoroughly studied yet. In the EU, drugs come into contact with the environment through wastewater and sewage sludge, while production plants are secondary sources [3–6].

In the last decades, drug treatment has sharply increased, especially among the older population, and Losartan and Irbesartan are among the most prescribed antihypertensive medicines [7–9]. They can pose a more significant threat than other substances because, as drugs, they are designed to be effective at low concentrations and because they are left unscathed by wastewater treatment plants [10], making their removal and monitoring of the utmost importance.

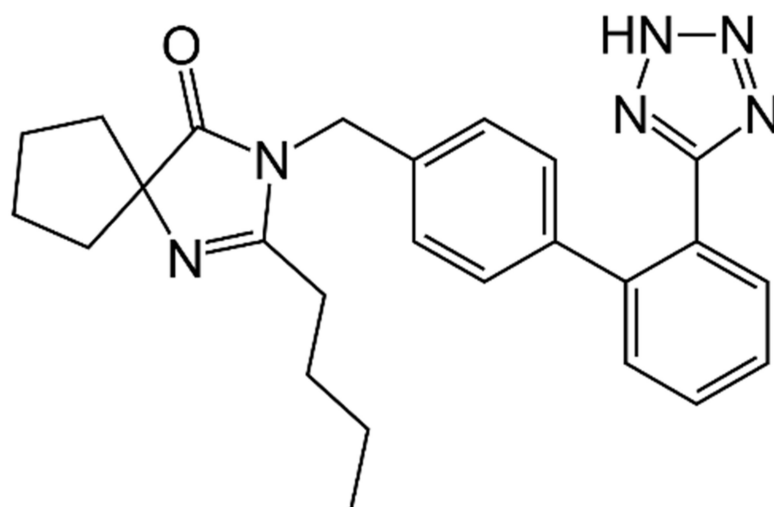


Figure 1. Molecular structure of Irbesartan.

High-Performance Liquid Chromatography (HPLC), coupled with a UV detector or MS/MS spectrometry, is the primary analytical technique used to investigate sartans in drug formulations or biological and environmental samples [11–15]. These techniques are time-consuming, can be expensive, often require a large quantity of solvents, and are not suitable for in situ analysis. Ultra-Performance Liquid Chromatography (UPLC) has been proposed as an alternative to HPLC because of the lesser volumes of solvents needed [11].

Electrochemical methods have rarely been investigated, using mainly Hanging Drop Mercury Electrode (HDME). For example, Gupta et al. [16] developed a voltammetric method for determining Irbesartan in pharmaceutical formulations. By applying Differential-Pulse Voltammetry (DPV), a cathodic peak appeared at -1.4 V (vs. saturated calomel electrode, SCE), corresponding to the reduction of the C=N double bond of the tetrazolyl moiety. A similar method was also proposed for determining Irbesartan in pharmaceuticals and biological fluids [17] by using both Differential-Pulse Voltammetry (DPV) and Square-Wave Voltammetry (SWV), obtaining a detection limit of about 0.7 μ M. A more sensitive voltammetric determination was that reported by El-Desoky et al. [18] for dosing Irbesartan in human blood and pharmaceutical formulations; a very low detection limit, 2 nM, was achieved by applying square-wave adsorptive cathodic stripping voltammetry.

For years, mercury electrodes have been the leading choice for voltammetric measurements. However, in the last decades, environmental and safety concerns have restricted their application and encouraged the exploration of more eco-friendly materials less toxic than mercury, with more possibilities for flow and in-situ analysis [19]. In this scenario, screen-printed electrodes (SPEs) had significant growth in demand since the screen-printing technique offers advantages in terms of versatility, cost-effectiveness and ease of use [20]. Moreover, screen-printed electrodes are among the most suitable sensors for in situ analysis thanks to their low power needs, rapid response, and good sensitivity [21]. The excellent versatility of the SPEs is driven primarily by the numerous ways in which the electrodes can be modified. For example, the composition of the inks may be changed by adding different substances, such as complexing ligands, metal particles, polymers, or enzymes. Otherwise, modifying the manufactured electrodes by depositing on their surface metal films, nanoparticles, biological material, and polymeric films is possible [22].

Molecularly imprinted polymers (MIPs) have been employed in various analytical methods, including electrode surface modification for potentiometric or voltammetric measurements to improve selectivity; a gain in sensitivity was also verified several times [23]. MIP-based sensors are some of the most popular approaches for detecting different classes of analytes, primarily biological molecules. MIPs embody a class of synthetic receptors that mimic natural antibody–antigen interactions, i.e., the “lock and key” mechanism to

bind the target analyte selectively [24]. For MIP synthesis, monomers are polymerized in the presence of a target molecule (the so-termed template), which is removed after the polymeric network is formed. The template removal leaves cavities in the polymers that mirror the target molecule's shape [25].

In this view, they possess the high selectivity and specificity of biological receptors but with the added advantage of being artificial polymers, much more stable and readily adaptable for the modification of electrode surfaces [26].

The development of MIPs tailored to screen-printed electrodes has accelerated the shift from bulky conventional techniques to low-cost and rapid-sensing devices for in-field analyses [27]. Recently, several studies have been published regarding the development of MIP-based screen-printed electrodes for both the voltammetric and potentiometric sensing of environmental contaminants, emerging pollutants, or biomolecules [28–40].

Following this trend, a MIP-modified screen-printed carbon electrode for Irbesartan voltammetric sensing is developed. The MIP's prepolymeric composition and the experimental parameters for the analysis by Square-Wave Voltammetry (SWV) are optimized using a Design of Experiments (DoE) approach. The reliability of the proposed method is proved by the analyses of tap water samples fortified with the drug.

2. Materials and Methods

2.1. Reagents and Instruments

Methacrylic acid (MMA) and ethylene glycol dimethacrylate (EGDMA) were purchased from Merk Life Science S.r.l. (Milano, Italy) and filtered with an aluminum oxide column to remove stabilizers.

Moreover, 2,2-azobisisobutyronitrile (AIBN), glacial acetic acid $\geq 99\%$, methanol, sodium acetate trihydrate, Irbesartan, and Losartan were used as obtained from Merk Life Science S.r.l. (Milano, Italy). Solutions for the electrode surface characterization were prepared using sodium chloride, potassium chloride, and potassium hexacyanoferrate (III) (Merk Life Science S.r.l., Milano, Italy). Three-electrode screen-printed cells with a graphite-ink working electrode, Ag/AgCl-ink pseudo-reference electrode, and a graphite-ink counter electrode were produced by Topflight Italia SPA (Vidigulfo, Pavia-Italy). Tap water from the lab sink (Department of Chemistry, University of Pavia, Italy) was used to prepare fortified samples.

Voltammetric analyses and impedance spectroscopy measurements were performed by the potentiostat/galvanostat EmStat4s-PalmSens BV (Houten-The Netherlands). The pH of buffers and solutions was checked by a pH-meter Mettler Toledo mod. SevenMulti, equipped with a combined glass electrode InLab Pro (Mettler Toledo, Milan, Italy).

2.2. Prepolymeric Mixture and Modification of the Working Electrode Surface

The prepolymeric solution was prepared according to the optimized procedure by mixing Irbesartan (IRB), MMA, and EGDMA with a molar ratio of 1:4:10 and adding the minimum amount of methanol to facilitate and completely dissolve all components. The mixture was deaerated with a gentle flow of N_2 for 5 min; then AIBN was included, and the mixture was sonicated until obtaining a limpid solution.

An equal prepolymeric mixture not containing Irbesartan was prepared for functionalizing the working electrode with the NIP (non-imprinted polymer).

Each screen-printed cell (SPC) was washed with methanol and left to dry at room temperature under a hood. A small volume of the prepolymeric mixture (3 μ L MIP or NIP mixture) was drop-coated on the cleaned surface of the working electrode. The thermal polymerization was carried out in a thermostatic oven at 60 °C overnight.

The SPC was then subjected to 7 cleaning cycles by immersion for 1 h in 10 mL of a mixture of glacial acetic acid $\geq 99\%$ /methanol = 1/4 to remove the template (IRB) and unreacted monomers. The so-cleaned functionalized SPC was stored at room temperature and hydrated in ultrapure water for 10 min before use.

2.3. Characterization of the Working Electrode Surface

The electrochemically active area was measured before and after the working graphite electrode surface modification with MIP or NIP.

It was determined by cyclic voltammetry (CV) in 5 mM $K_4Fe(CN)_6$ /0.1 M KCl solution at pH 7.2 as an electrochemical probe ($E_{start} = -1$ V, $E_{end} = +1$ V, scan rate $0.025 \div 0.5$ V/s).

The square root of the scan rate vs. the intensity of the anodic or cathodic peak was plotted; from the slope (K), the effective area is obtained through the modified Randles–Sevcik’s equation [35,41]:

$$A = \frac{K}{2.69 \cdot 10^5 \cdot n^{3/2} \cdot D^{1/2} \cdot C} \quad (1)$$

D and C are, respectively, the diffusion coefficient ($D = 3.09 \cdot 10^{-6}$ cm²/s) and the concentration ($C = 5$ mM) of the electrochemical probe $K_4Fe(CN)_6$; n is the number of the electrons acquired for the reduction of the electrochemical probe, i.e., $n = 1$ according to the reaction: $Fe(CN)_6^{3-} + e^- \rightarrow Fe(CN)_6^{4-}$.

The Electrochemical Impedance Spectroscopy (EIS) experiments were carried out in 15 mL of 5 mM $K_4Fe(CN)_6$ /0.1 M KCl solution at pH 7.2 (electrochemical probe solution), registering the electrochemical impedance from 100 kHz to 10 mHz, and a signal amplitude of 50 mV. The analyses were performed for unmodified screen-printed cells (bare) as well as for those modified with MIP and NIP.

2.4. Irbesartan Determination by Square-Wave Voltammetry (SWV)

Irbesartan was detected by Square-Wave Voltammetry (SWV) in 15 mL of 0.1 M acetate buffer solutions at pH 5.5, gently stirring and applying the experimental conditions, optimized through a Design of Experiments (DoE) approach, as reported in Table 1.

Table 1. Experimental conditions, optimized through a Design of Experiments (DoE) approach, for Irbesartan analyses by SWV.

Parameters	Bare Electrode	MIP-/NIP-Modified Electrode
E_{start} (V)	+1.0	+1.0
E_{end} (V)	−1.5	−1.5
Frequency (Hz)	50	1.0
Impulse amplitude (V)	0.1	0.05
Equilibration time (s)	120	300

3. Results

3.1. Screen-Printed Working Electrode Functionalization

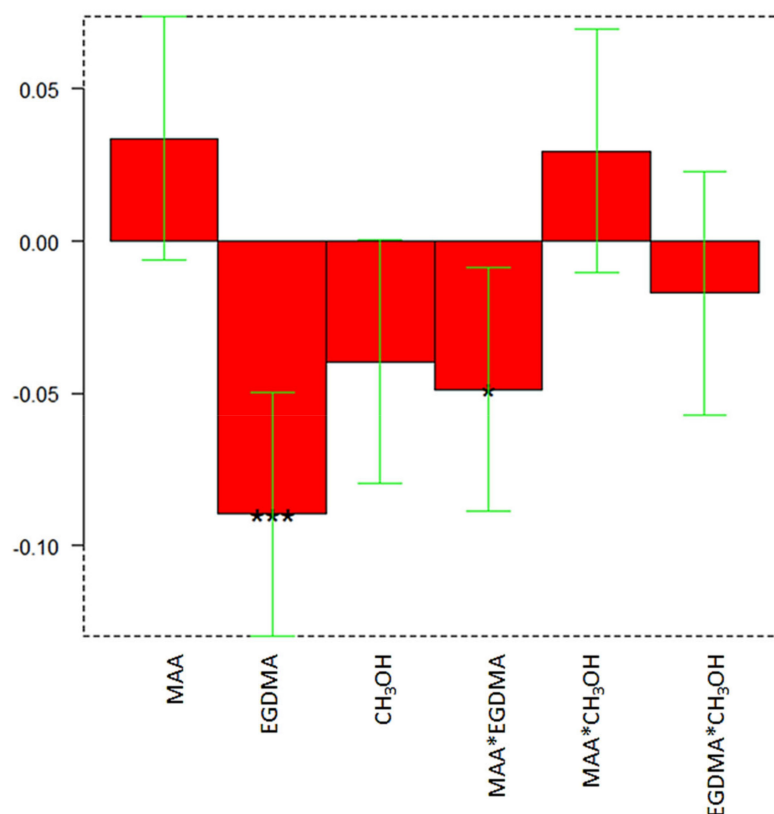
When using screen-printed cells, the first concern is the modification only of the working electrode surface, avoiding the possible compromise of the counter and pseudo-reference electrodes. Therefore, a good option was a drop-coating of a small volume of the prepolymeric mixture. After testing volumes from 1 to 5 μ L, the correct quantity was determined to be 3 μ L, enough to coat the working electrode surface and leave the other electrodes unaltered.

The second step was the optimization of the prepolymeric mixture composition aiming to obtain the best compromise in terms of sensitivity and selectivity; thus, a simple full factorial design 2^3 was applied. Table 2 summarizes the parameters under investigation and the corresponding minimum and maximum levels. The current peak (i_p , μ A) obtained by SWV analysis was evaluated as the response. The data were processed using the open-source software CAT (Chemometric Agile Tool) [42]. The graph of Figure 2 shows the significance of the model’s coefficients.

Table 2. Optimization of the prepolymeric mixture by a Full Factorial Design 2^3 : level definitions for the parameters considered, keeping constant the Irbesartan content (0.05 mmol).

Parameter	Minimum Level (−1)	Maximum Level (+1)
MAA ¹ (mmol)	0.1	0.2
EGDMA ² (mmol)	0.5	1.0
CH ₃ OH ³ (mL)	0.4	0.8

¹ MAA = methacrylic acid (functional monomer). ² EGDMA = ethylene glycol dimethacrylate (cross-linker).
³ CH₃OH = methanol (solvent).

**Figure 2.** Experimental design to optimize the prepolymeric mixture: coefficients plot. The greatest values and little black stars (regardless of the sign) suggest a significant influence of the respective parameter or interaction and significance (* $p \leq 0.05$, *** $p \leq 0.001$).

The model equation can be written as follows:

$$i_p = b_0 + b_1[\text{MAA}] + b_2[\text{EGDMA}] + b_3[\text{CH}_3\text{OH}] + b_{12}[\text{MAA}][\text{EGDMA}] + b_{13}[\text{MAA}][\text{CH}_3\text{OH}] + b_{23}[\text{EGDMA}][\text{CH}_3\text{OH}] \quad (2)$$

The values of the coefficient and their significance are summarized in Table 3.

Table 3. Coefficients and significance (* $p \leq 0.05$, *** $p \leq 0.001$) calculated for the optimization of the prepolymeric mixture by a Full Factorial Design 2^3 .

Coefficient	Value	Significance
b_0	0.3462	
b_1	0.0337	
b_2	−0.0896	***
b_3	−0.0396	
b_{12}	−0.0487	*
b_{13}	0.0296	
b_{23}	−0.0171	

The coefficient plot of Figure 1 highlights that the significant parameters/interactions are the mmol of EGDMA and the interaction between mmol MAA and mmol EGDMA; conversely, the solvent volume is irrelevant. The mmol of EGMA has a negative effect on the current peak, so it has to be set at the minimum value ($-1 = 0.5$ mmol). The interaction between mmol MAA and mmol EGDMA presents a significant negative effect on the response; thus, setting mmol EGDMA at the minimum value ($-1 = 0.5$ mmol), mmol MAA has to be set at the highest value ($+1 = 0.2$ mmol).

Six replicates at the center point [0 0 0] were set up, and the average value, standard deviation, and confidence interval (CI) at a 95% confidence level are reported in Table 4. The predicted value fits into the confidence interval; thus, the model is validated.

Table 4. Optimization of the prepolymeric mixture by a Full Factorial Design 2^3 : model validation by six replicates at the center point [0 0 0], i.e., 0.15 mmol MAA, 0.75 mmol EGDMA and 0.6 mL CH_3OH . CI = confidence interval at 95% confidence level.

	<i>ip</i> (μA)
Average	0.33
Standard deviation	0.02
Upper bound CI	0.35
Lower bound CI	0.31
Predicted response (b_0)	0.3462

Therefore, the optimal prepolymeric mixture had the following composition:

IRB: MAA: EGDMA = 0.05 mmol:0.2 mmol:0.5 mmol = 1:4:10. As previously stated, the volume of methanol is irrelevant, and the maximum value of 0.8 mL was selected to be sure to solubilize all the mixture components well.

3.2. Characterization of the Working Electrode Surface

3.2.1. Electrode Active Area

The electrode area was calculated for the bare, MIP-, and NIP-modified electrodes. Each obtained value was compared to the theoretical one. In order to define the active area, cyclic voltammetric measurements were performed in an electrochemical probe solution at different scan rates, and the reduction or oxidation peak height was plotted against the square root of the scan rate. The slope of the obtained straight line (K) was entered in Randles–Sevcik’s equation (Equation (1), Section 2.3) to obtain the active area’s value.

Since both reduction and oxidation peaks were analyzed, Table 5 shows the averages of the two area values.

Table 5. Active areas calculated by Randles–Sevcik’s equation (average of the values obtained by plotting the anodic and the cathodic peak of the CV vs. the square root of the scan rate. Electrochemical probe: 5 mM $\text{K}_4\text{Fe}(\text{CN})_6$ /0.1 M KCl solution at pH 7.2). The number in parenthesis is the standard deviation on the last digit.

	Active Area (mm^2)
Bare electrode	12.3(3)
MIP-modified electrode	9.59(2)
NIP-modified electrode	8.80(3)
Theoretical	12.6

The values in Table 5 show that the active area decreases when the electrode is coated with a non-conductive polymer. As we expected, the active area of the MIP-modified electrode is higher than that of the NIP-modified electrode; this behavior is due to the cavities in the molecularly imprinted polymer, which are, on the contrary, absent in the NIP.

3.2.2. Electrochemical Impedance Spectroscopy (EIS)

Electrochemical Impedance Spectroscopy is a technique used to characterize the electrodic surface; in particular, the polymers' non-conductive nature may be verified. The measurements were performed in 15 mL of 5 mM $K_4Fe(CN)_6$ /0.1 M KCl solution. The NIP-modified electrode, the MIP-modified electrode after the template removal, and the same electrode recharged with the analyte were analyzed. Figure 3 shows the Nyquist plots obtained for each electrode.

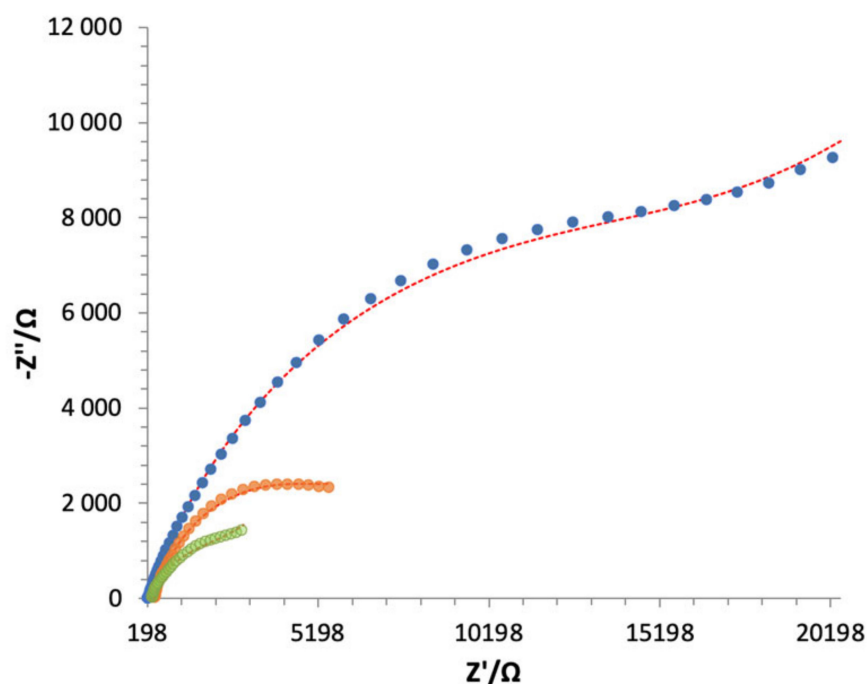


Figure 3. Nyquist plots of the NIP-modified electrode (blue bullets) and MIP-modified electrode after the template removal (empty green bullets) and after contact with IRB solution (empty orange bullets). Electrochemical probe: 5 mM $K_4Fe(CN)_6$ /0.1 M KCl solution at pH 7.2.

As can be observed from the Nyquist plot, the resistance of the electrode surface increases passing from the washed to the recharged polymer that modifies the screen-printed cell. This behavior may be related to the presence of the analyte that plugs the pores and prevents the electric charges from reaching the electrode surface. This behavior is amplified using the NIP, which has a lower porosity than the MIP.

The Nyquist plot may be explained as recurring to a Randles' equivalent circuit describing the obtained trends, reported in Figure 4.

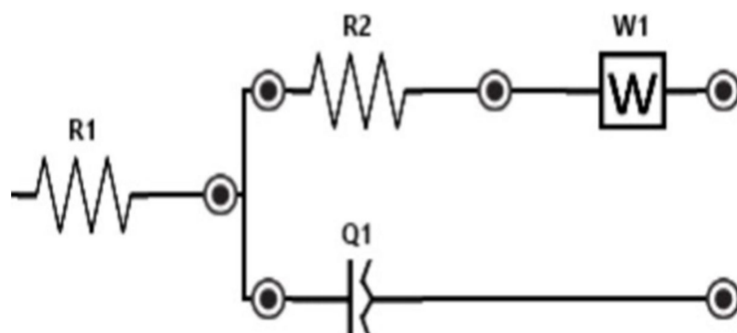


Figure 4. Randles' equivalent circuit describing the Nyquist plot of Figure 3.

The Randles equivalent circuit of Figure 4 comprises three different circuital elements. R1 is the resistance of the solution, R2 is the resistance to the charge transfer of the electrode/electrolyte interface, and W is the Warburg component that describes the diffusive processes, while Q1 represents the constant phase element. Q1 (or constant phase element, CPE) describes the accumulation of ions on an inhomogeneous electrode surface, and it is used instead of the classic C_{dl} (double-layer capacitance).

The fitting curves in Figure 3 were calculated according to Randles's equivalent circuit over-described. The Nyquist plots with their fitting for each electrode are shown in the Supplementary Materials.

The fitting error was obtained using the following Equation (3) [43]:

$$E\% = \frac{\sqrt{\sum \frac{(fit-exp)^2}{exp^2}}}{N} \quad (3)$$

fit stands for fitting value, *exp* for experimental value, and N for the number of points taken into account. The calculated fitting errors are reported in Table 6.

Table 6. Fitting errors for the Nyquist curves of Figure 3, calculated using Equation (3).

	E%
MIP-modified electrode after the template removal	0.8
MIP-modified electrode after contact with IRB solution	3.7
NIP-modified electrode	2.4

3.3. Irbesartan Determination by Square-Wave Voltammetry (SWV): Optimization of the Procedure, Calibration and Real Sample Analysis

Once the screen-printed cell (SPC) was modified with the molecularly imprinted polymer, and before its use for the voltammetric measurements, it was washed several times with a mixture of methanol/glacial acetic acid $\geq 99\% = 1/4$ to remove the template molecule. Calibration measurements were performed on both the bare electrode and the MIP-modified one. The experiments were carried out in 30 mL of 0.1 M acetate buffer at pH 5.5 and applying SWV; the signal was recorded after an equilibration time of 120 or 300 s, respectively, for the bare electrode or the MIP-/NIP-modified one. For the MIP-modified electrodes, the equilibration time corresponds to the incubation period necessary for the Irbesartan molecule to reach the cavities of the polymeric film. The experimental conditions for both electrodes were optimized by a full factorial design 2^3 ; the current peak (i_p , μA) was evaluated as the response. The levels of the variables, the coefficient plots, and their significance and model equations are reported in the Supplementary Materials. Table 1 (Section 2.4) shows the optimized SWV experimental conditions for bare and MIP-/NIP-modified electrodes.

Figure 5 shows the calibrations obtained for the electrodes modified with MIP and NIP by plotting the cathodic current peak (i_p , μA) vs. Irbesartan concentration (μM). As expected from the experiments performed with the NIP-modified electrode, only a residual current independent of the Irbesartan concentration was registered.

The straight line's equations of the calibrations reported in Figure 5 are:

$i_p [\mu A] = 1.30(3) + 6.9(2) \cdot [IRB, \mu M]$ $R^2 = 0.994$ for the MIP-modified electrode;
 $i_p [\mu A] = 1.23(3) - 0.4(3) \cdot [IRB, \mu M]$ $R^2 = 0.168$ for the NIP-modified electrode
 (number in round brackets is the standard deviation of the last digit).

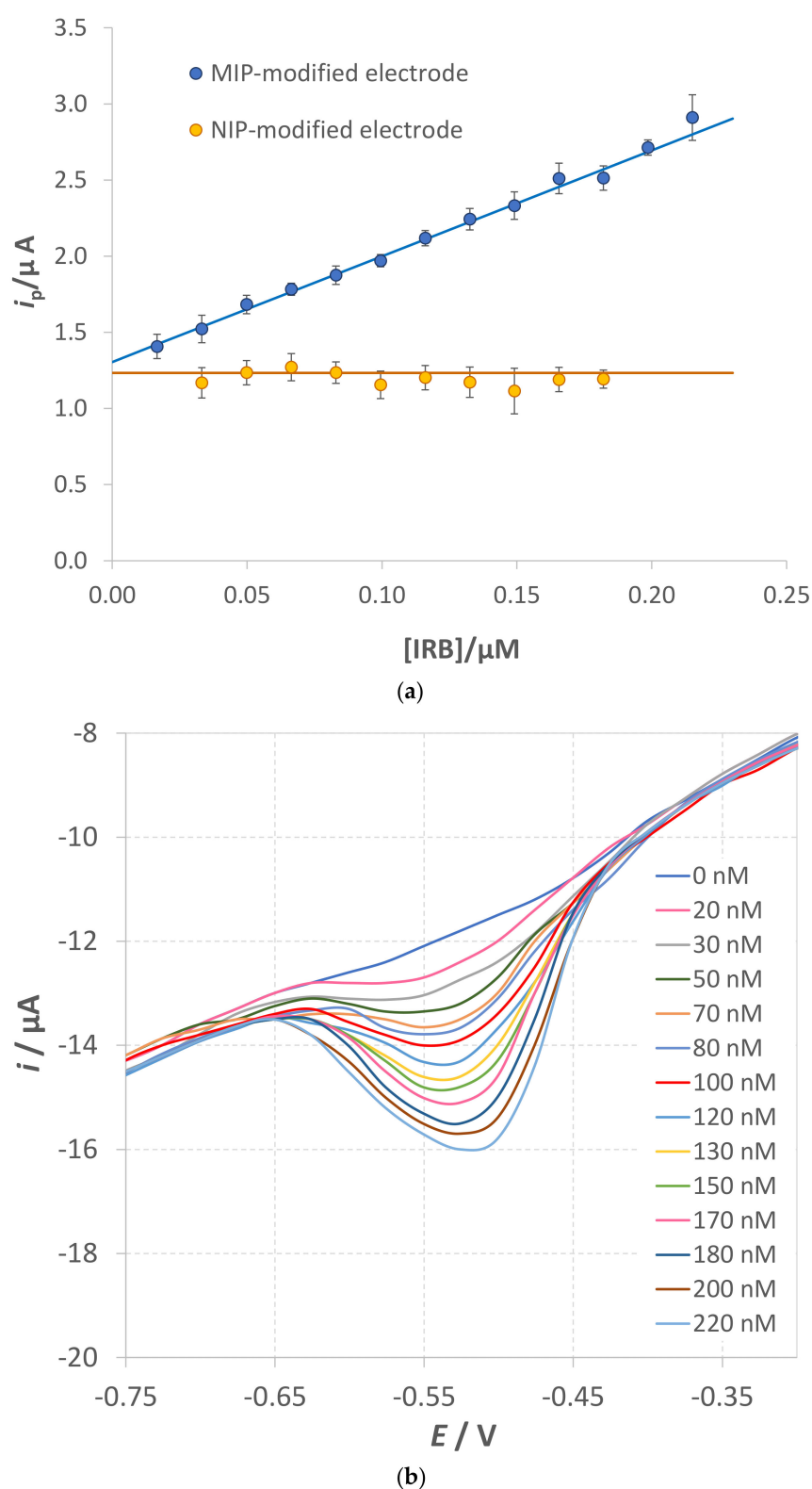


Figure 5. (a) Calibration curves of the MIP-modified electrode (blue dots) and NIP-modified electrode (orange dots). (b) SW voltammograms of the calibration curve for one MIP-modified electrode.

Experimental conditions: SWV in 0.1 M acetate buffer pH 5.5; E_{start} : +1 V; E_{end} : -1.5 V; frequency: 1 Hz; amplitude: 0.05 V; equilibration time: 300 s. The error bars correspond to the standard deviation of the measurements performed with three electrodes.

The detection and quantification limits were calculated by the following Equations (4) and (5):

$$\text{LOD} = \frac{3.3 \cdot s_{y/x}}{\text{slope}} \quad (4)$$

$$\text{LOQ} = \frac{10 \cdot s_{y/x}}{\text{slope}} \quad (5)$$

where $s_{y/x}$ is the standard deviation of y -residuals (i.e., the random errors in the y -direction); this value can be assumed not significantly different from the standard deviation of replicate measurements of blank solutions [44].

For the MIP-modified electrodes, the values expressed as the average of the results obtained from three different calibration curves using three screen-printed cells were LOD 0.012(3) μM and LOQ 0.03(1) μM .

Some calibrations were also performed with the bare screen-printed electrode applying the optimized operative conditions reported in Table 1. In this case, the linearity range was slightly wider than that achieved with the MIP-modified electrode, but higher LOD and LOQ were obtained.

Table 7 summarizes the analytical performances for both modified and non-modified electrodes.

Table 7. Limits of Detection (LOD), Limits of Quantification (LOQ) and Limits of Linearity (LOL) for bare and MIP-modified screen-printed electrodes. LOD and LOQ are reported as the average of results obtained from three different calibration curves. The number in parenthesis is the standard deviation.

	Bare	MIP
Sensitivity ($\mu\text{A}/\mu\text{M}$)	5.4(1)	6.9(2)
LOD (μM)	0.09(2)	0.012(3)
LOQ (μM)	0.26(5)	0.03(1)
LOL (μM)	0.26–4	0.03–0.3

The applicability of the MIP-based screen-printed electrode for environmental analyses was tested by using it to detect Irbesartan in fortified tap water samples. Table 8 shows the recovery% and error% obtained; they were calculated by Equations (6) and (7), respectively.

$$\text{Recovery \%} = 100 \cdot \frac{C_{\text{experimental}}}{C_{\text{nominal}}} \quad (6)$$

$$\text{Error \%} = 100 \cdot \frac{(C_{\text{nominal}} - C_{\text{experimental}})}{C_{\text{nominal}}} \quad (7)$$

Table 8. Recovery% and Error% using SPC-bare and SPC-MIP of tap water adjusted to pH 5.5 and fortified with different concentrations of Irbesartan.

	$C_{\text{nominal}}/\text{M}$	$C_{\text{experimental}}/\text{M}$	Recovery%	Error%
MIP-modified electrode	$3.6 \cdot 10^{-7}$	$3.37(6) \cdot 10^{-7}$	93.6	−6.4
Bare electrode	$3.6 \cdot 10^{-7}$	$1.2(1) \cdot 10^{-7}$	33.3	−66.7
MIP-modified electrode	$1.4 \cdot 10^{-7}$	$1.3(2) \cdot 10^{-7}$	92.8	−7.1
Bare electrode	$1.4 \cdot 10^{-7}$	$3.9(5) \cdot 10^{-7}$	278	178

Table 8 shows good recoveries and a maximum error of 7.1% for the MIP-modified electrode, while the bare one is definitely not a selective sensor since the recoveries were unsatisfactory. The bad results obtained with the bare electrode could be due to the interference of electroactive substances present in the real samples; the presence of the

specific MIP's cavities reduces the chance of such interferences reaching the electrode surface, making more accurate measurements possible.

In Table 9, the analytical performances of the MIP-based screen-printed electrode are compared with those of other electrochemical methods for sartan detection reported in the literature.

Table 9. Comparison of the analytical performances of electrochemical methods for Irbesartan detection.

Method	Electrode	LOL μM	LOD μM	Ref.
SW-AdCSV ^a	HDME	0.003–0.5	0.0009	[18]
SWV ^b	HDME	0.2–3.0	0.15	[45]
DPV ^c	HDME	30–5700	0.53	[16]
DPV ^c	HDME	8–100	0.77	[17]
SWV ^b	HDME	8–100	0.60	[17]
SWV ^b	MIP-modified screen-printed electrode	0.03–0.3	0.012	This work

^a SW-AdCSV = Square-Wave Adsorptive Cathodic Stripping Voltammetry. ^b SWV = Square-Wave Voltammetry. ^c DPV = Differential-Pulse Voltammetry.

3.4. Interference Test

The selectivity of the MIP-modified electrode was tested in solutions containing Losartan (see the molecular structure in Figure 6).

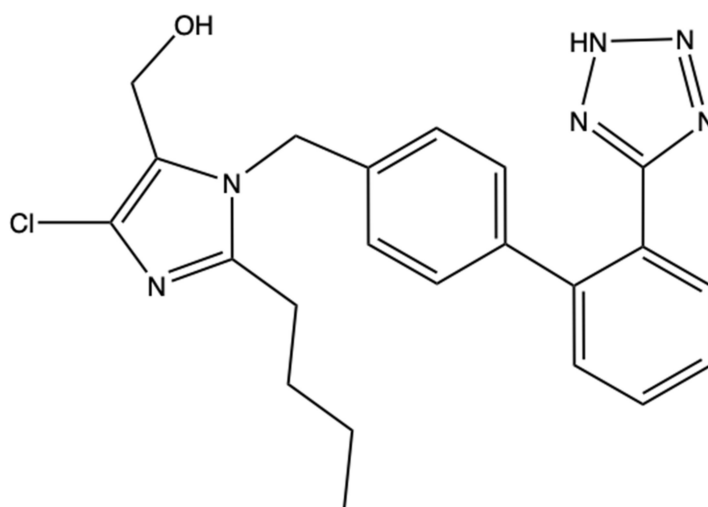


Figure 6. Molecular structure of Losartan.

As can be observed from Figures 1 and 5, the molecular structures of Irbesartan and Losartan are very similar; for this reason, the comparable behavior of the MIP-modified electrode for both analytes can be expected. SWV performed the calibration measurements in the same conditions described for the Irbesartan experiments. As an example, the equation of the straight line obtained from a calibration curve with an MIP-modified electrode in Losartan solutions is reported below:

$$i_p (\mu\text{A}) = 1.4 \cdot C_{\text{Los}} (\mu\text{M}) + 0.2 \quad R^2 = 0.970$$

The sensitivity of the sensor for 1.4 μA/μM of Losartan is five times lower than that obtained for Irbesartan, but is still significant; therefore, effectively, the electrode also allows the dosage of this molecule. The fact that the sensor responds non-specifically but selectively to sartans of a similar structure may be advantageous for application in the analysis of environmental samples contaminated by a mixture of these substances.

4. Conclusions

This paper describes a screen-printed voltammetric sensor for the determination of Irbesartan, obtained by modifying the graphite working electrode surface with a molecularly imprinted polymer (MIP).

Before and after modification, the working electrode surface was characterized by EIS and the active area was calculated. The results of both methods demonstrated the covering of the surface with the MIP layer.

From the calibration measurements performed under optimized conditions, a LOD of 0.012(3) μM and a LOQ of 0.04(1) μM were obtained.

The applicability of the sensor for environmental analyses was tested by detecting Irbesartan in fortified tap water samples obtaining good recoveries.

Selectivity tests were also undertaken using Losartan as an interferent. The sensor's sensitivity for this sartan was five times lower than that obtained for Irbesartan, but was still significant. It can then be concluded that the MIP-modified electrode responds non-specifically but selectively to sartans of similar structures. This experimental evidence was predictable given the very similar structure of the two compounds but can be considered advantageous for applying the sensor in the analyses of environmental samples containing a mixture of these emerging contaminants.

Supplementary Materials: The following supporting information can be downloaded at: <https://www.mdpi.com/article/10.3390/chemosensors10120517/s1>, Figure S1: DoE to optimize SWV experimental conditions for the bare electrode. The greatest values and little black stars (regardless of the sign) suggest a significant influence of the respective parameter or interaction and significance (* $p \leq 0.05$, ** $p \leq 0.01$, *** $p \leq 0.001$); Figure S2: DoE to optimize SWV experimental conditions for the MIP-/NIP-modified electrode. The greatest values and little black stars (regardless of the sign) suggest a significant influence of the respective parameter or interaction and significance (* $p \leq 0.05$, ** $p \leq 0.01$, *** $p \leq 0.001$); Figure S3: Nyquist plots of the MIP-modified electrode after the template removal. Electrochemical probe: 5 mM K₄Fe(CN)₆/0.1 M KCl solution at pH 7.2; Figure S4: Nyquist plots of the cleaned MIP-modified electrode after contact with IRB solution. Electrochemical probe: 5 mM K₄Fe(CN)₆/0.1 M KCl solution at pH 7.2. Figure S5: Nyquist plots of the NIP-modified electrode. Electrochemical probe: 5 mM K₄Fe(CN)₆/0.1 M KCl solution at pH 7.2. Table S1: Optimization of the SWV experimental conditions for the bare electrode by a Full Factorial Design 2³: level definitions for the parameters considered; Table S2: Coefficients and significance (* $p \leq 0.05$, ** $p \leq 0.01$, *** $p \leq 0.001$) calculated for the optimization of the SWV experimental conditions for the bare electrode by a Full Factorial Design 2³; Table S3: Optimization of the SWV experimental conditions for the bare electrode by a Full Factorial Design 2³: model validation by six replicates of the center point [0 0 0], i.e., Fz = 25 Hz, A = 75 mV and t = 210 s. CI = confidence interval at 95% confidence level; Table S4: Optimization of the SWV experimental conditions for the MIP-/NIP-modified electrode by a Full Factorial Design 2³: level definitions for the parameters considered; Table S5: Coefficients and significance (* $p \leq 0.05$, ** $p \leq 0.01$, *** $p \leq 0.001$) calculated for the optimization of the SWV experimental conditions for the MIP-/NIP-modified electrode by a Full Factorial Design 2³; Table S6: Optimization of the SWV experimental conditions for the MIP-/NIP-modified electrode by a Full Factorial Design 2³: model validation by six replicates of the center point [0 0 0], i.e., Fz = 25 Hz, A = 75 mV and t = 120 s. CI = confidence interval at 95% confidence level.

Author Contributions: Conceptualization, G.A. and R.R.; methodology, G.A. and R.R.; investigation, R.R. and C.Z.; data curation, G.A. and C.Z.; writing—original draft preparation, G.A. and C.Z.; writing—review and editing, L.R.M., R.R. and R.B. All authors have read and agreed to the published version of the manuscript.

Funding: This research received no external funding.

Institutional Review Board Statement: Not applicable.

Informed Consent Statement: Not applicable.

Data Availability Statement: Not applicable.

Acknowledgments: We thank Topflight Italia (S.P.A.) for providing us with screen-printed cells free of charge.

Conflicts of Interest: The authors declare no conflict of interest.

References

1. Croom, K.F.; Curran, M.P.; Goa, K.L.; Perry, C.M. Irbesartan. *Drugs* **2004**, *64*, 999–1028. [\[CrossRef\]](#) [\[PubMed\]](#)
2. Darwish, I.A.; Darwish, H.W.; Bakheit, A.H.; Al-Kahtani, H.M.; Alanazi, Z. Irbesartan (a comprehensive profile). *Profiles Drug Subst. Excip. Relat. Methodol.* **2021**, *46*, 185–272. [\[CrossRef\]](#) [\[PubMed\]](#)
3. Petrović, M.; Hernando, M.D.; Díaz-Cruz, M.S.; Barceló, D. Liquid chromatography–tandem mass spectrometry for the analysis of pharmaceutical residues in environmental samples: A review. *J. Chromatogr. A* **2005**, *1067*, 1–14. [\[CrossRef\]](#) [\[PubMed\]](#)
4. Malmborg, J.; Magnér, J. Pharmaceutical residues in sewage sludge: Effect of sanitization and anaerobic digestion. *J. Environ. Manag.* **2015**, *153*, 1–10. [\[CrossRef\]](#) [\[PubMed\]](#)
5. Gracia-Lor, E.; Sancho, J.V.; Serrano, R.; Hernández, F. Occurrence and removal of pharmaceuticals in wastewater treatment plants at the Spanish Mediterranean area of Valencia. *Chemosphere* **2012**, *87*, 453–462. [\[CrossRef\]](#)
6. Boix, C.; Ibáñez, M.; Fabregat-Safont, D.; Morales, E.; Pastor, L.; Sancho, J.V.; Sánchez-Ramírez, J.E.; Hernández, F. Behaviour of emerging contaminants in sewage sludge after anaerobic digestion. *Chemosphere* **2016**, *163*, 296–304. [\[CrossRef\]](#)
7. Lewis, E.J.; Lewis, J.B. Treatment of diabetic nephropathy with angiotensin II receptor antagonist. *Clin. Exp. Nephrol.* **2003**, *7*, 1–8. [\[CrossRef\]](#)
8. Lewis, E.J.; Hunsicker, L.G.; Clarke, W.R.; Berl, T.; Pohl, M.A.; Lewis, J.B.; Ritz, E.; Atkins, R.C.; Rohde, R.; Raz, I.; et al. Renoprotective Effect of the Angiotensin-Receptor Antagonist Irbesartan in Patients with Nephropathy Due to Type 2 Diabetes. *N. Engl. J. Med.* **2001**, *345*, 851–860. [\[CrossRef\]](#)
9. Brenner, B.M.; Cooper, M.E.; De Zeeuw, D.; Keane, W.F.; Mitch, W.E.; Parving, H.-H.; Remuzzi, G.; Snapinn, S.M.; Zhang, Z.; Shahinfar, S. Effects of Losartan on Renal and Cardiovascular Outcomes in Patients with Type 2 Diabetes and Nephropathy. *N. Engl. J. Med.* **2001**, *345*, 861–869. [\[CrossRef\]](#)
10. Loos, R.; Carvalho, R.; António, D.C.; Comero, S.; Locoro, G.; Tavazzi, S.; Paracchini, B.; Ghiani, M.; Lettieri, T.; Blaha, L.; et al. EU-wide monitoring survey on emerging polar organic contaminants in wastewater treatment plant effluents. *Water Res.* **2013**, *47*, 6475–6487. [\[CrossRef\]](#)
11. Muszalska, I.; Sobczak, A.; Dolhań, A.; Jelińska, A. Analysis of Sartans: A Review. *J. Pharm. Sci.* **2014**, *103*, 2–28. [\[CrossRef\]](#)
12. Castro, G.; Rodríguez, I.; Ramil, M.; Cela, R. Selective determination of sartan drugs in environmental water samples by mixed-mode solid-phase extraction and liquid chromatography tandem mass spectrometry. *Chemosphere* **2019**, *224*, 562–571. [\[CrossRef\]](#)
13. Nalini, C.N.; Nivedhitha, M. A review on analytical methods of irbesartan and its combinations in pharmaceutical dosage forms. *Curr. Pharm. Anal.* **2020**, *16*, 1020–1029. [\[CrossRef\]](#)
14. Yogeesh, C.S.; Sowmya, H.G.; Babu, J.G.C. Analytical method development and validation of irbesartan: Review. *Eur. J. Pharm. Med. Res.* **2019**, *6*, 235–238.
15. Virani, P.; Rajaniti, S.; Hasumati, R.; Jain, V. Irbesartan: A review on analytical method and its determination in pharmaceuticals and biological matrix. *Pharm. Anal. Qual. Assur.* **2014**, *2014*, 1–8.
16. Gupta, V.K.; Jain, R.; Agarwal, S.; Mishra, R.; Dwivedi, A. Electrochemical determination of antihypertensive drug irbesartan in pharmaceuticals. *Anal. Biochem.* **2011**, *410*, 266–271. [\[CrossRef\]](#)
17. Bozal, B.; Doğan-Topal, B.; Uslu, B.; Özkan, S.A.; Aboul-Enein, H.Y. Quantitative Analysis of Irbesartan in Pharmaceuticals and Human Biological Fluids by Voltammetry. *Anal. Lett.* **2009**, *42*, 2322–2338. [\[CrossRef\]](#)
18. El-Desoky, H.S.; Ghoneim, M.M.; Habazy, A.D. Voltammetry of irbesartan drug in pharmaceutical formulations and human blood: Quantification and pharmacokinetic studies. *J. Braz. Chem. Soc.* **2011**, *22*, 239–247. [\[CrossRef\]](#)
19. Ariño, C.; Serrano, N.; Díaz-Cruz, J.M.; Esteban, M. Voltammetric determination of metal ions beyond mercury electrodes. A review. *Anal. Chim. Acta* **2017**, *990*, 11–53. [\[CrossRef\]](#)
20. Suresh, R.R.; Lakshmanakumar, M.; Arockia Jayalatha, J.B.B.; Rajan, K.S.; Sethuraman, S.; Krishnan, U.M.; Rayappan, J.B.B. Fabrication of screen-printed electrodes: Opportunities and challenges. *J. Mater. Sci.* **2021**, *56*, 8951–9006. [\[CrossRef\]](#)
21. Li, M.; Li, Y.-T.; Li, D.-W.; Long, Y.-T. Recent developments and applications of screen-printed electrodes in environmental assays—A review. *Anal. Chim. Acta* **2012**, *734*, 31–44. [\[CrossRef\]](#) [\[PubMed\]](#)
22. Renedo, O.D.; Alonso-Lomillo, M.A.; Martínez, M.A. Recent developments in the field of screen-printed electrodes and their related applications. *Talanta* **2007**, *73*, 202–219. [\[CrossRef\]](#) [\[PubMed\]](#)
23. Cervini, P.; Cavalheiro, É.T.G. Strategies for Preparation of Molecularly Imprinted Polymers Modified Electrodes and Their Application in Electroanalysis: A Review. *Anal. Lett.* **2012**, *45*, 297–313. [\[CrossRef\]](#)
24. Hasseb, A.A.; Ghani, N.D.T.A.; Shehab, O.R.; El Nashar, R.M. Application of molecularly imprinted polymers for electrochemical detection of some important biomedical markers and pathogens. *Curr. Opin. Electrochem.* **2022**, *31*, 100848. [\[CrossRef\]](#)
25. Scheller, F.W.; Zhang, X.; Yarman, A.; Wollenberger, U.; Gyurcsányi, R.E. Molecularly imprinted polymer-based electrochemical sensors for biopolymers. *Curr. Opin. Electrochem.* **2019**, *14*, 53–59. [\[CrossRef\]](#)

26. Feroz, M.; Vadgama, P. Molecular Imprinted Polymer Modified Electrochemical Sensors for Small Drug Analysis: Progress to Practical Application. *Electroanalysis* **2020**, *32*, 2361–2386. [CrossRef]
27. Ferrari, A.G.-M.; Rowley-Neale, S.J.; Banks, C.E. Screen-printed electrodes: Transitioning the laboratory in-to-the field. *Talanta Open* **2021**, *3*, 100032. [CrossRef]
28. Ekomo, V.M.; Branger, C.; Bikanga, R.; Florea, A.-M.; Istamboulie, G.; Calas-Blanchard, C.; Noguer, T.; Sarbu, A.; Brisset, H. Detection of Bisphenol A in aqueous medium by screen printed carbon electrodes incorporating electrochemical molecularly imprinted polymers. *Biosens. Bioelectron.* **2018**, *112*, 156–161. [CrossRef]
29. Jamieson, O.; Soares, T.C.C.; De Faria, B.A.; Hudson, A.; Mecozzi, F.; Rowley-Neale, S.J.; Banks, C.E.; Gruber, J.; Novakovic, K.; Peeters, M.; et al. Screen printed electrode based detection systems for the antibiotic amoxicillin in aqueous samples utilizing molecularly imprinted polymers as synthetic receptors. *Chemosensors* **2020**, *8*, 5. [CrossRef]
30. El-Sharif, H.F.; Patel, S.; Ndunda, E.N.; Reddy, S.M. Electrochemical detection of dioctyl phthalate using molecularly imprinted polymer modified screen-printed electrodes. *Anal. Chim. Acta* **2022**, *1196*, 339547. [CrossRef]
31. Johari-Ahar, M.; Karami, P.; Ghanei, M.; Afkhami, A.; Bagheri, H. Development of a molecularly imprinted polymer tailored on disposable screen-printed electrodes for dual detection of EGFR and VEGF using nano-liposomal amplification strategy. *Biosens. Bioelectron.* **2018**, *107*, 26–33. [CrossRef]
32. Ayankojo, A.G.; Reut, J.; Öpik, A.; Syritski, V. Sulfamethizole-imprinted polymer on screen-printed electrodes: Towards the design of a portable environmental sensor. *Sens. Actuators B Chem.* **2020**, *320*, 128600. [CrossRef]
33. Sharif, H.E.; Dennison, S.R.; Tully, M.; Crossley, S.; Mwangi, W.; Bailey, D.; Graham, S.P.; Reddy, S.M. Evaluation of electropolymerized molecularly imprinted polymers (E-MIPs) on disposable electrodes for detection of SARS-CoV-2 in saliva. *Anal. Chim. Acta* **2022**, *1206*, 339777. [CrossRef]
34. Lee, M.-H.; Thomas, J.L.; Liu, W.-C.; Zhang, Z.-X.; Liu, B.-D.; Yang, C.-H.; Lin, H.-Y. A multichannel system integrating molecularly imprinted conductive polymers for ultrasensitive voltammetric determination of four steroid hormones in urine. *Microchim. Acta* **2019**, *186*, 695. [CrossRef]
35. Pesavento, M.; Merli, D.; Biesuz, R.; Alberti, G.; Marchetti, S.; Milanese, C. A MIP-based low-cost electrochemical sensor for 2-furaldehyde detection in beverages. *Anal. Chim. Acta* **2021**, *1142*, 201–210. [CrossRef]
36. Alberti, G.; Zanoni, C.; Spina, S.; Magnaghi, L.R.; Biesuz, R. MIP-Based Screen-Printed Potentiometric Cell for Atrazine Sensing. *Chemosensors* **2022**, *10*, 339. [CrossRef]
37. Balayan, S.; Chauhan, N.; Chandra, R.; Jain, U. Electrochemical Based C-Reactive Protein (CRP) Sensing Through Molecularly Imprinted Polymer (MIP) Pore Structure Coupled with Bi-Metallic Tuned Screen-Printed Electrode. *Biointerface Res. Appl. Chem.* **2022**, *6*, 38.
38. Gonçalves, M.D.L.; Truta, L.A.; Sales, M.G.F.; Moreira, F.T. Electrochemical point-of care (PoC) determination of interleukin-6 (IL-6) using a pyrrole (Py) molecularly imprinted polymer (MIP) on a carbon-screen printed electrode (C-SPE). *Anal. Lett.* **2021**, *54*, 2611–2623. [CrossRef]
39. Khosrokhavar, R.; Motaharian, A.; Hosseini, M.R.M.; Mohammadsadegh, S. Screen-printed carbon electrode (SPCE) modified by molecularly imprinted polymer (MIP) nanoparticles and graphene nanosheets for determination of sertraline antidepressant drug. *Microchem. J.* **2020**, *159*, 105348. [CrossRef]
40. Motaharian, A.; Hosseini, M.R.M.; Naseri, K. Determination of psychotropic drug chlorpromazine using screen printed carbon electrodes modified with novel MIP-MWCNTs nano-composite prepared by suspension polymerization method. *Sens. Actuators B Chem.* **2019**, *288*, 356–362. [CrossRef]
41. Burak, D.; Emregul, E.; Emregul, K.C. Copper–zinc alloy nanoparticle based enzyme-free superoxide radical sensing on a screen-printed electrode. *Talanta* **2015**, *134*, 206–214. [CrossRef]
42. Chemometric Agile Tool (CAT). Available online: <http://www.gruppochemiometria.it/index.php/software/19-download-the-r-based-chemometric-software> (accessed on 27 October 2022).
43. Saxena, R.; Srivastava, S. An insight into impedimetric immunosensor and its electrical equivalent circuit. *Sens. Actuators B Chem.* **2019**, *297*, 126780. [CrossRef]
44. Miller, J.N.; Miller, J.C. Calibration methods in instrumental analysis: Regression and correlation. In *Statistics and Chemometrics for Analytical Chemistry*, 6th ed.; Pearson Education Limited: Harlow Essex, UK, 2010; pp. 124–126.
45. Palabiyık, M.; Dogan, A.; Süslü, I. Simultaneous Determination of Amlodipine and Irbesartan in Their Pharmaceutical Formulations by Square-Wave Voltammetry. *Comb. Chem. High Throughput Screen.* **2022**, *25*, 241–251. [CrossRef] [PubMed]